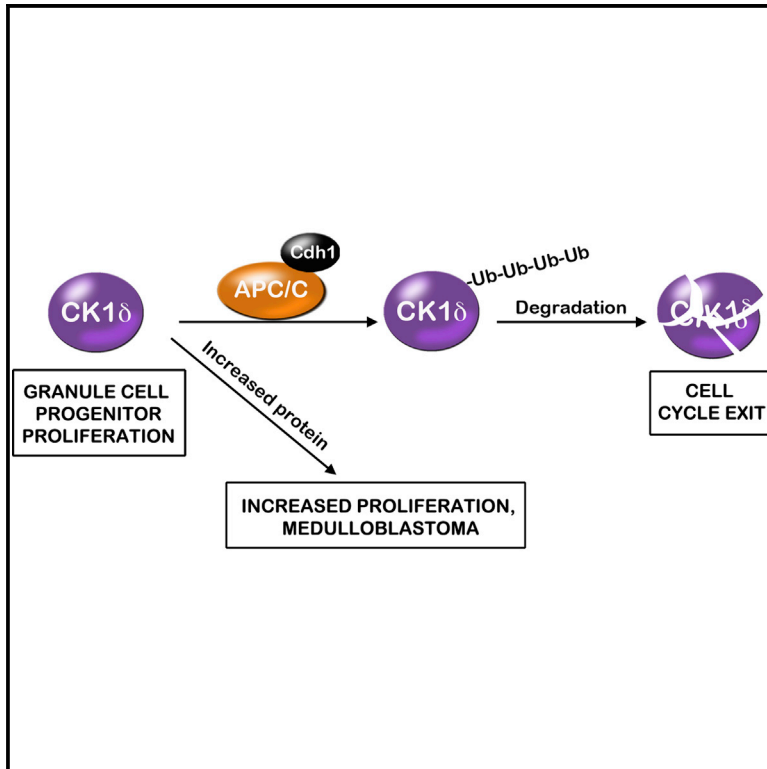


Casein Kinase 1 δ Is an APC/C^{Cdh1} Substrate that Regulates Cerebellar Granule Cell Neurogenesis

Graphical Abstract



Authors

Clara Penas, Eve-Ellen Govek, ..., Mary E. Hatten, Nagi G. Ayad

Correspondence

nayad@miami.edu

In Brief

Penas et al. find that CK1 δ controls cerebellar granule cell progenitor (GCP) proliferation. They also find that the ubiquitin ligase anaphase-promoting complex/cyclosome (APC/C) targets CK1 δ for degradation by the proteasome. APC/C-dependent degradation of CK1 δ may be linked to GCP cell-cycle exit and neurogenesis in the developing CNS.

Highlights

- CK1 δ is required for cerebellar granule cell progenitor neurogenesis
- CK1 δ inhibition or CK1 δ knockdown induces cell-cycle arrest
- CK1 δ is targeted for degradation via the anaphase-promoting complex/cyclosome
- CK1 δ destruction is required for cell-cycle exit



Casein Kinase 1 δ Is an APC/C^{Cdh1} Substrate that Regulates Cerebellar Granule Cell Neurogenesis

Clara Penas,¹ Eve-Ellen Govek,² Yin Fang,² Vimal Ramachandran,¹ Mark Daniel,¹ Weiping Wang,³ Marie E. Maloof,¹ Ronald J. Rahaim,⁴ Mathieu Bibian,⁴ Daisuke Kawauchi,⁵ David Finkelstein,⁶ Jeng-Liang Han,⁴ Jun Long,⁷ Bin Li,⁷ David J. Robbins,⁷ Marcos Malumbres,⁸ Martine F. Roussel,⁵ William R. Roush,⁴ Mary E. Hatten,² and Nagi G. Ayad^{1,*}

¹Center for Therapeutic Innovation, Department of Psychiatry and Behavioral Sciences, University of Miami, Miami, FL 33136, USA

²Laboratory of Developmental Neurobiology, The Rockefeller University, New York, NY 10065, USA

³Department of Systems Biology, Harvard Medical School, Boston, MA 02115, USA

⁴Department of Chemistry, Scripps Florida, Jupiter, FL 33458, USA

⁵Department of Tumor Cell Biology

⁶Department of Computational Biology

St. Jude Children's Research Hospital, Memphis, TN 38105, USA

⁷Departments of Surgery and Biochemistry and Molecular Biology, Molecular Oncology Program, University of Miami Miller School of Medicine, Miami, FL 33136, USA

⁸Cell Division and Cancer Group, Spanish National Cancer Research Centre, 28029 Madrid, Spain

*Correspondence: nayad@miami.edu

<http://dx.doi.org/10.1016/j.celrep.2015.03.016>

This is an open access article under the CC BY-NC-ND license (<http://creativecommons.org/licenses/by-nc-nd/4.0/>).

SUMMARY

Although casein kinase 1 δ (CK1 δ) is at the center of multiple signaling pathways, its role in the expansion of CNS progenitor cells is unknown. Using mouse cerebellar granule cell progenitors (GCPs) as a model for brain neurogenesis, we demonstrate that the loss of CK1 δ or treatment of GCPs with a highly selective small molecule inhibits GCP expansion. In contrast, CK1 δ overexpression increases GCP proliferation. Thus, CK1 δ appears to regulate GCP neurogenesis. CK1 δ is targeted for proteolysis via the anaphase-promoting complex/cyclosome (APC/C^{Cdh1}) ubiquitin ligase, and conditional deletion of the APC/C^{Cdh1} activator *Cdh1* in cerebellar GCPs results in higher levels of CK1 δ . APC/C^{Cdh1} also downregulates CK1 δ during cell-cycle exit. Therefore, we conclude that APC/C^{Cdh1} controls CK1 δ levels to balance proliferation and cell-cycle exit in the developing CNS. Similar studies in medulloblastoma cells showed that CK1 δ holds promise as a therapeutic target.

INTRODUCTION

The casein kinase 1 (CK1) family of monomeric serine/threonine protein kinases is evolutionarily conserved in eukaryotes. Seven members have been identified in mammals: α , β , δ , ϵ , γ 1, γ 2, and γ 3 (Gross and Anderson, 1998; Knippschild et al., 2005; Rowles et al., 1991; Zhai et al., 1995). These kinases target a broad spectrum of substrates to control diverse biological processes, e.g., signal transduction, circadian rhythms, nuclear import, DNA repair, apoptosis, spindle assembly, vesicle trafficking, neurite outgrowth, and primary cilia formation (Behrend et al., 2000; Be-

yaert et al., 1995; Cheong and Virshup, 2011; Desagher et al., 2001; Gault et al., 2012; Gross and Anderson, 1998; Knippschild et al., 2005; Petronczki et al., 2006; Price, 2006; Vielhaber and Virshup, 2001). However, whether CK1 mediates the generation of specific classes of CNS neurons is unknown (Löhler et al., 2009).

During brain development, cerebellar granule cell progenitors (GCPs) expand to produce the most numerous neuronal population in the brain. This proliferation is followed by cell-cycle exit and differentiation. Thus, we predict that drivers of GCP expansion and proliferation are downregulated during cell-cycle exit. However, others have postulated that CK1 isoforms are unregulated (Knippschild et al., 2005). Whether CK1 δ is downregulated during GCP cell-cycle exit is unknown. CK1 δ is targeted for ubiquitin-mediated proteolysis via the anaphase-promoting complex/cyclosome (APC/C^{Cdh1}). Conditional deletion of the APC/C activator *Cdh1* in the developing cerebellum increases CK1 δ levels in vivo. Furthermore, CK1 δ stabilization increases GCP proliferation, suggesting a crucial role of APC-dependent CK1 δ degradation during cell-cycle exit. Moreover, downregulation of CK1 δ in GCPs increases the level of Wee1, a cell-cycle inhibitory kinase. Wee1 turnover increases Cdk1 activity and mitotic entry (Owens et al., 2010; Smith et al., 2007; Watanabe et al., 2004, 2005). We previously demonstrated that CK1 δ controls Wee1 degradation (Penas et al., 2014), which is important for cell proliferation.

APC/C^{Cdh1} is a tumor suppressor; thus, APC/C-dependent degradation of CK1 δ is most likely deregulated in some cancers. GCPs are thought to give rise to medulloblastoma, the most common malignant pediatric brain tumor. Several GCP developmental pathways are deregulated in medulloblastoma, including WNT, SHH, MYC, and some undefined pathways (Hatten and Roussel, 2011). Mutations in the SHH receptors *Patched* (*PTCH1*), *Suppressor of fused* (*SUFU*), and *Smoothened* (*SMO*) are associated with medulloblastoma and other malignancies (Evans et al., 1991; Hallahan et al., 2004; Svärd

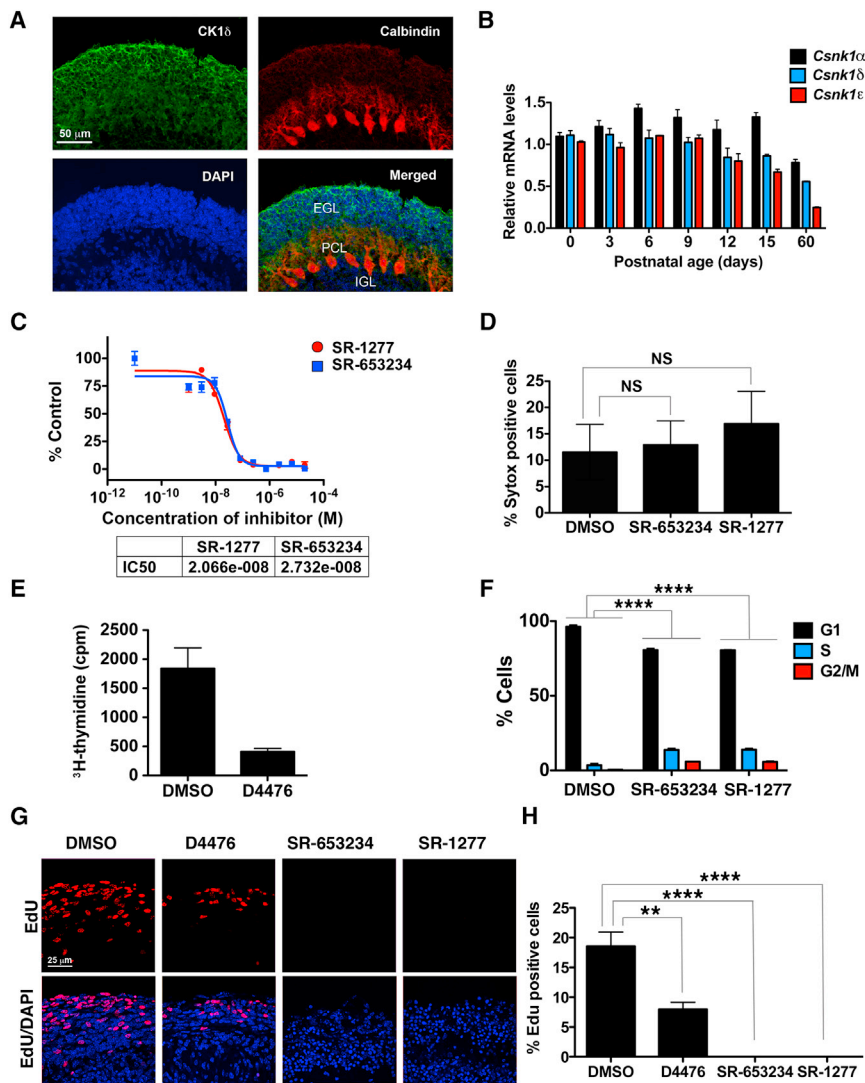


Figure 1. CK1 δ Expression in Postnatal GCPs and Control of GCP Proliferation In Vitro and Ex Vivo

(A) Cerebellar sections from P8 pups were stained with antibodies against CK1 δ (green) or calbindin (red) and DAPI (blue).

(B) CK1 α , CK1 δ , and CK1 ϵ mRNA were amplified by qRT-PCR, and fold change in gene expression in postnatal mouse cerebellum was determined by normalizing to GAPDH values relative to control.

(C) GCPs were incubated for 24 hr with increasing concentrations of SR-653234 or SR-1277, and the amount of proliferation was determined by ³H-thymidine incorporation. Results were plotted relative to that seen in the DMSO control.

(D) GCPs were treated with 100 nM SR-653234 or SR-1277 for 24 hr, and then Sytox and Hoechst staining was performed (NS, not significant, as determined by one-way ANOVA and Dunnett multiple comparisons test).

(E and F) (E) D4476 (20 μ M) reduces GCP proliferation and (F) SR-653234 (100 nM) and SR-1277 (100 nM) increase the percentage of GCPs in the S or G2/M phase. GCPs were treated for 24 hr with the indicated compounds or DMSO, and the proportion of cells in each cell-cycle phase was determined by PI-FACS.

(G) Organotypic cerebellar slices were treated with SR-1277 (100 nM), SR-653234 (100 nM), D4476 (20 μ M), or DMSO for 1 hr, after which EdU was added to the media for 20 hr. Slices were stained with EdU (red) and the nuclear marker DAPI (blue).

(H) Quantification of (G). Results are shown as the average values of three independent experiments and are represented as the mean \pm SEM (*p < 0.05, **p < 0.001, ***p < 0.001, ****p < 0.0001).

et al., 2006; Taylor et al., 2002; Yauch et al., 2009). Group 3 (G3) medulloblastoma, the most aggressive form of the disease, is associated with MYC overexpression (Cho et al., 2011; Ellison et al., 2011; Northcott et al., 2011; Pfister et al., 2009). Recent sequencing studies have demonstrated CK1 δ overexpression in G3 medulloblastoma, suggesting a role for CK1 isoforms in some medulloblastoma subgroups (Gibson et al., 2010; Jones et al., 2012; Northcott et al., 2012; Pugh et al., 2012; Robinson et al., 2012).

CK1 δ is expressed in mouse cerebellum (Löhler et al., 2009), an opportune model for CNS neurogenesis. Here we investigated the role of CK1 δ in GCP expansion in the developing CNS. We also examined whether proteolytic degradation via APC/C^{Cdh1} regulates CK1 δ in vitro and in vivo. Finally, we measured the levels of CK1 δ in medulloblastoma cells relative to that in control GCPs, and we determined whether the cells are responsive to CK1 δ inhibition in vivo in allograft and intracranial xenograft mouse models. Our results indicate that CK1 δ may be a novel therapeutic target in medulloblastoma.

RESULTS

CK1 δ Is Required for Cerebellar GCP Proliferation

During normal brain development, GCPs expand to generate 45 billion granule neurons; the adult human brain contains 100 billion neurons (Roussel and Hatten, 2011). Because CK1 δ is expressed postnatally in cerebellar GCPs (Figures 1A and 1B), we examined whether it is involved in GCP neurogenesis and cell-cycle exit. Purified GCPs are used to study proliferation and differentiation because they proliferate effectively in cell aggregates in suspension. Conversely, they exit the cell cycle and differentiate when plated on poly-D-lysine/laminin-coated plates.

To determine whether CK1 δ inhibition affects GCP proliferation, we treated cells in suspension with SR-653234 or SR-1277, two highly specific, potent small-molecule inhibitors of CK1 δ (Bibian et al., 2013; Penas et al., 2014). We measured the rate of proliferation of purified GCPs in the presence and absence of SR-653234 or SR-1277 by ³H-thymidine uptake

(Figure 1C). Both compounds inhibited GCP proliferation with a similar IC_{50} (Figure 1C), but neither caused cell death (Figure 1D). Treatment with the well-characterized CK1 δ inhibitor D4476 also reduced GCP proliferation in vitro (Figure 1E). The proportion of GCPs in S phase was higher in cells treated with SR-653234 or SR-1277 (13.7% and 18.9%, respectively) than it was in DMSO-treated controls (3.4%), as were those in G2/M (SR-653234, 5.8%; SR-1277, 5.6%; DMSO, 0.1%), as determined by propidium iodide fluorescence-activated cell sorting (PI-FACS) (Figure 1F). We did not observe cells containing DNA content lower than 2N (sub-G1 phase), which further confirmed that the inhibitor concentrations used did not kill the cells (Figure 1F). These results suggest that pharmacologic inhibition of CK1 δ induces GCP cell-cycle arrest in the S or G2/M phases.

To test whether CK1 δ is required for GCP proliferation in an ex vivo model, we treated slices of postnatal cerebellar tissue with D4476, SR-653234, or SR-1277 (Figure 1G). The cerebellar GCP is a well-studied model of proliferation; dividing cells are restricted to the external germinal layer. Postmitotic GCPs localize beneath mitotic cells, initiate differentiation by extending parallel fiber axons, and migrate along the radial fibers of Bergmann glia (Edmondson and Hatten, 1987; Rakic, 1972). Thus, the position of labeled GCPs in organotypic slices of developing cerebellum indicates their proliferation status. EdU assays of organotypic slices of postnatal cerebellum in culture (Tomoda et al., 1999) showed less EdU uptake in D4476-treated slices and dramatically less in SR-653234- or SR-1277-treated cells relative to the DMSO-treated control (Figure 1G). EdU incorporation is a measure of proliferation; therefore, these results suggest that CK1 δ inhibition disrupts GCP proliferation ex vivo.

CK1 δ Knockdown Reduces Cerebellar GCP Proliferation

To validate the requirement of CK1 δ in GCP proliferation, we depleted CK1 δ levels by small interfering RNA (siRNA)-mediated knockdown. Electroporation of purified GCPs with two different siRNAs effectively decreased CK1 δ mRNA and qRT-PCR analysis shows that CK1 ϵ or CK1 α levels were unchanged (Figures 2A and 2B). SHH is a potent mitogen of GCP proliferation; therefore, we tested whether depleting the level of CK1 δ affected the rate of SHH-mediated incorporation of EdU into GCPs. CK1 δ knockdown decreased the levels of the proliferative markers phospho-Histone H3 and cyclin B1 in the absence or presence of SHH (Figures 2B and 2C). Furthermore, EdU incorporation was reduced in GCPs electroporated with CK1 δ -specific siRNAs, relative to control siRNA (Figures 2E and 2F). In contrast, CK1 ϵ depletion did not affect EdU incorporation (Figure 2D). These results indicate that CK1 δ is required for GCP proliferation in vitro, and reducing its levels attenuates SHH-induced mitogenesis.

To determine whether CK1 δ is important for GCP proliferation ex vivo, we conditionally deleted CK1 δ in cerebellar GCPs by using *Atoh1-Cre*, a GCP-specific Cre driver, and measured 3H -thymidine incorporation in purified GCPs. GCPs purified from *Tg(Atoh1-Cre)+;Csnk1d^{fl/fl}* mice had a slightly lower rate of 3H -thymidine incorporation than did GCPs purified from *Tg(Atoh1-Cre)-;Csnk1d^{fl/fl}* mice. However, we observed a more pronounced decrease in proliferation in GCPs from *Tg(Atoh1-Cre)+;Csnk1d^{fl/fl}* mice treated with SHH (Figure 2G). Cyclin B1

and phospho-Histone 3 levels were also lower after CK1 δ deletion (Figure 2H), suggesting that GCP expansion is reduced upon CK1 δ deletion ex vivo. Wee1 levels were upregulated after CK1 δ deletion (Figures 2H and 2I); thus, increased Wee1 levels may also limit GCP expansion. Together, these results demonstrate that CK1 δ functions in cerebellar GCP proliferation in vitro and ex vivo.

CK1 δ Inhibition Affects GCP Cell-Cycle Progression

To better understand the role of CK1 δ in GCP proliferation, we analyzed the levels of cell-cycle regulators after pharmacologic inhibition of CK1 δ in purified GCPs. GCPs were treated with SHH, SR-1277, or both for 24 or 48 hr and processed for qRT-PCR analysis. We first analyzed the levels of various cyclins that are essential regulators of cyclin-dependent kinases and cell-cycle transitions in multiple model systems, including GCPs. SR-1277 decreased the mRNA levels of cyclins *A1* (*Ccna1*), *B1* (*Ccnb1*), *D2* (*Ccnd2*), and *E1* (*Ccne1*) induced by SHH (Figure 3A), but did not alter that of the cyclin-dependent kinase inhibitors *p21^{Cip1}* (*Cdkn1a*) and *p27^{Kip1}* (*Cdkn1b*). Similar results were found after electroporation of purified GCPs with specific CK1 δ siRNAs (Figure 3B). Incubation with SR-1277 or electroporation with CK1 δ siRNAs also decreased the levels of the main effectors of the SHH pathway, *Gli1* and *Gli2*, in GCPs (Figures S1A and S1B). These results confirmed that specific inhibition or decreased levels of CK1 δ arrest the GCP cell cycle.

APC/C^{Cdh1} Specifically Targets CK1 δ for Proteolysis

Many cell-cycle regulators are subject to ubiquitin-dependent proteolysis; therefore, we asked whether CK1 δ is degraded via this process. APC/C^{Cdh1} recognizes many substrates via a canonical destruction (D-box) motif that contains a minimal consensus sequence of RXXL, where X is any amino acid. Cdh1 binding to RXXL motifs initiates ubiquitin transfer and subsequent ubiquitin-dependent substrate degradation (Barford, 2011; Owens and Hoyt, 2005; Song and Rape, 2011). We examined the protein sequence of all human CK1 isoforms for putative RXXL motifs. CK1 δ has two RXXL motifs, one at position 8 (RYRL; DB1) and one at position 193 (RDDL; DB2), that are evolutionarily conserved (Figure 4A).

We hypothesized that the putative D-box motifs in CK1 δ are functional and mediate recognition by APC/C^{Cdh1}. Deletion or mutation of bona fide D-boxes in previously reported APC/C^{Cdh1} substrates decreased Cdh1-dependent ubiquitination and degradation (Penas et al., 2012); therefore, we performed site-directed mutagenesis to produce versions of CK1 δ -V5 that had mutations in DB1 (Δ DB1), DB2 (Δ DB2), or both (Δ DB1 DB2). Both D-boxes were mutated with alanine substitutions of their respective arginine (R) and leucine (L) residues (Figure 4A). Several studies have shown that the D-box-dependent destruction of substrates can be ablated with RXXL-to-AXXA substitutions (Choi et al., 2008; King et al., 1996; Listovsky et al., 2004; Stewart and Fang, 2005; Zur and Brandeis, 2002).

We measured the in vitro degradation of wild-type or D-box-mutated CK1 δ in somatic HeLa cell extracts that were isolated from cells in early G1 phase, when APC/C^{Cdh1} is most active. Mutating DB1 or DB2 reduced CK1 δ destruction, but inactivating both D-boxes profoundly stabilized the protein (Figures 4B and

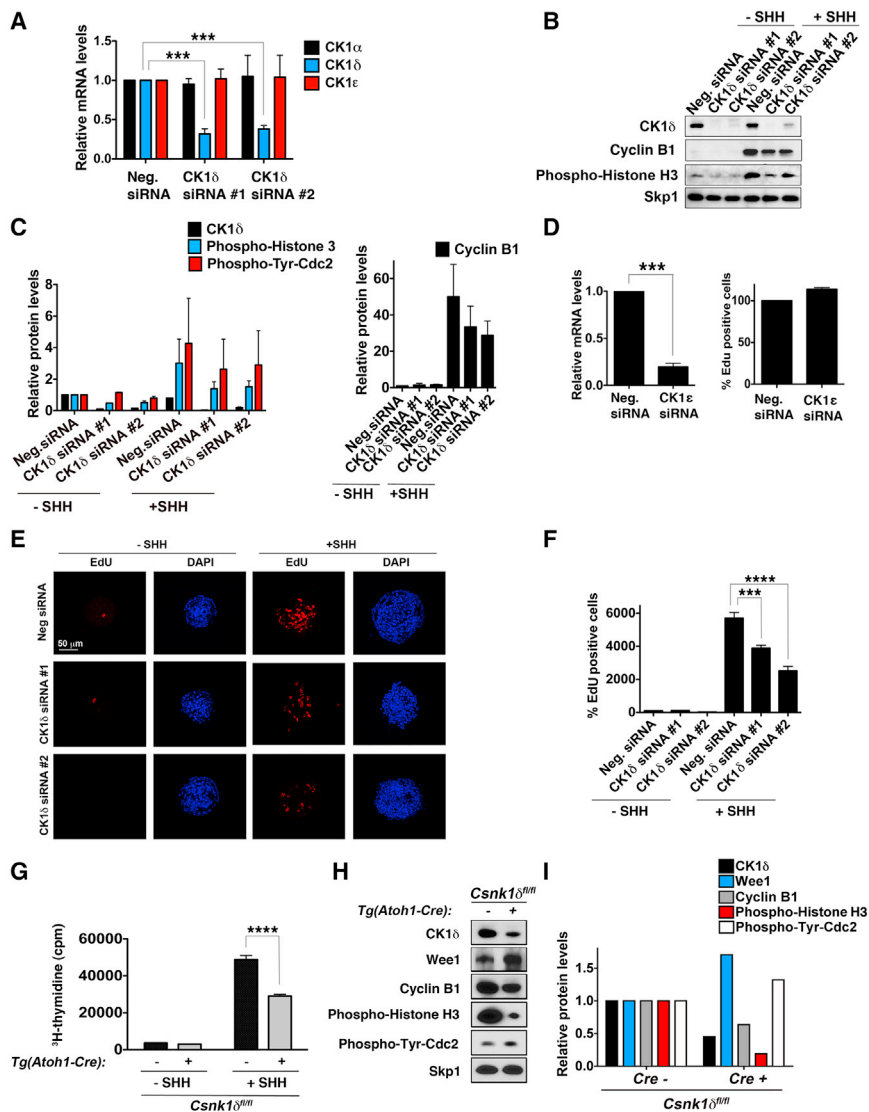


Figure 2. CK1 δ Knockdown Reduces GCP Proliferation In Vitro and Ex Vivo

(A) GCP cells electroporated with two different CK1 δ siRNAs were analyzed by qRT-PCR. CK1 δ was significantly knocked down, but CK1 α and CK1 ϵ levels were not altered. The mRNA was amplified by qRT-PCR, and the fold change in gene expression was determined by normalizing to GAPDH values relative to controls.

(B) After electroporation of GCPs with or without SHH (75 ng/ml), the levels of CK1 δ , cyclin B1, and phospho-Histone H3 were analyzed by immunoblotting with antibodies against the proteins. Skp1 served as a loading control. CK1 δ was knocked down by both siRNAs.

(C) Quantification of the amount of CK1 δ , phospho-Histone H3, phospho-Tyr-Cdk1 (a measure of Wee1 inhibition of Cdk1), and cyclin B1, relative to the loading control Skp1, after CK1 δ siRNA electroporation in GCPs from (B) is shown.

(D) GCPs electroporated with CK1 ϵ siRNA were analyzed by qRT-PCR. CK1 ϵ was significantly knocked down, but EdU uptake was not reduced in the presence of SHH. Levels are expressed as the percentage of EdU uptake in cells treated with the negative siRNA.

(E) CK1 δ siRNA electroporation reduces EdU uptake of GCPs in the presence of SHH. Proliferative GCP aggregates were stained with EdU (red) and the nuclear marker DAPI (blue).

(F) Quantification of the EdU incorporation in (E). Levels are expressed as a percentage compared to that in cells treated with the negative siRNA without SHH.

(G) GCPs isolated from *Csnk1d*-deleted mice proliferate less in the presence or absence of SHH. Purified GCPs were treated for 24 hr with the compounds, and then ³H-thymidine was added to the media for an additional 24 hr. Plots representing the amounts of ³H-thymidine incorporated by GCPs from CK1 δ -deleted or control mice are shown.

(H) GCPs purified from conditional *Csnk1d*-deleted mice have lower levels of CK1 δ , cyclin B1, and phospho-Histone H3, indicating decreased

proliferation. Representative immunoblots of CK1 δ , Wee1, cyclin B1, phospho-Histone H3, and phospho-Tyr-cdc2 relative to Skp1 are shown. (I) Quantification of the amount of CK1 δ , Wee1, phospho-Histone H3, phospho-Tyr-Cdc2, and cyclin B1 protein, relative to the loading control Skp1, in GCPs isolated from *Tg(Atoh1-Cre)+;Csnk1d^{fl/fl}* or *Tg(Atoh1-Cre)-;Csnk1d^{fl/fl}* mice from (H). Results are shown as the averages of three independent experiments and are represented as the mean \pm SEM (***p < 0.001, ****p < 0.0001).

4C). Furthermore, the degradation of wild-type CK1 δ was similarly inhibited by the 26S proteasome inhibitor MG132 (Kisselev et al., 2012), suggesting that D-box-mediated degradation of CK1 δ is ubiquitin pathway dependent (Figures 4D and 4E).

To test whether CK1 δ is an in vitro substrate of APC/C^{Cdh1}, we incubated immunopurified APC/C^{Cdh1} with CK1 δ , Ube2s, and ubiquitin. CK1 δ was robustly ubiquitinated via APC/C^{Cdh1} (Figures 4F–4H). To assess whether mutation of CK1 D-boxes reduced APC/C^{Cdh1}-mediated ubiquitination, we performed in vitro ubiquitination assays with purified G1 APC/C^{Cdh1} and in-vitro-translated, ³⁵S-labeled CK1 δ -V5 or CK1 δ -V5 D-box mutants as substrates. Each single mutant significantly reduced CK1 δ ubiquitination (Figures 4F and 4G), and the double mutant nearly abolished polyubiquitination. Consistent with this finding,

mutating both D-boxes stabilized CK1 δ more than inactivating either one independently (Figures 5A and 5B).

To determine whether Cdh1 depletion reduces CK1 δ turnover, we measured the degradation of CK1 isoforms in HeLa cells transfected with Cdh1 siRNA or control GFP siRNA. Although CK1 δ and cyclin B1 were degraded in cells transfected with GFP siRNA, they were stabilized in Cdh1-depleted cells; other CK1 isoforms did not degrade in the same manner (Figures 5C and 5D), suggesting that Cdh1 specifically targets CK1 δ . We previously described CK1 δ -dependent Wee1 turnover (Penas et al., 2014); thus, we predicted that Cdh1 controls the level of Wee1. Wee1 levels were upregulated when CK1 δ was downregulated (Figures S2A and S2B), and they were reduced even more when the CK1 δ D-box mutant was

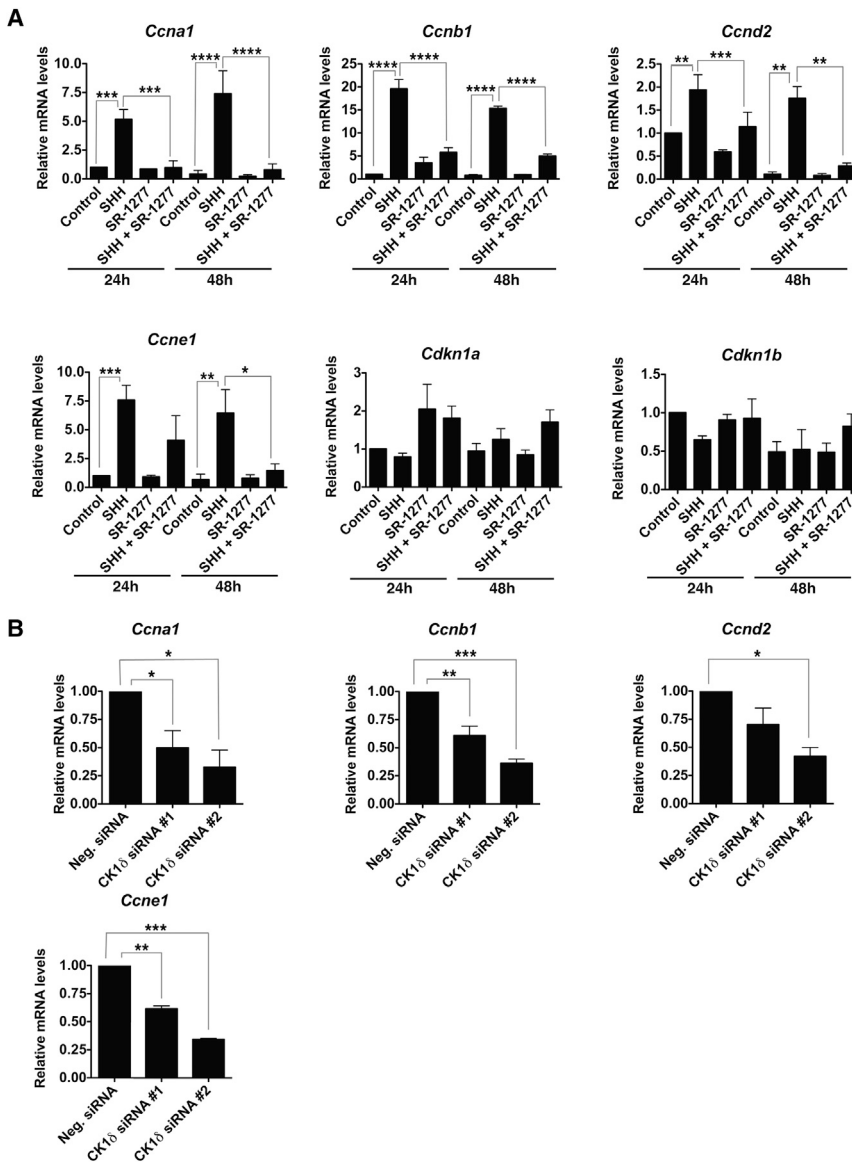


Figure 3. Inhibition or Knockdown of CK1 δ Reduces the mRNA Levels of Cell-Cycle Components

(A) SR-1277 (100 nM) decreases the expression of SHH-induced levels of *Ccna1*, *Ccnb1*, *Ccnd2*, *Ccne1*, *Cdkn1a*, and *Cdkn1b* mRNA in GCPs. GCPs were treated with SHH (75 ng/ml) and/or SR-1277 for 24 or 48 hr. The mRNA was amplified by qRT-PCR, and fold change in gene expression was determined by normalizing to *GAPDH* values relative to control samples.

(B) CK1 δ knockdown reduces the expression of *Ccna1*, *Ccnb1*, *Ccnd2*, and *Ccne1* mRNA levels in the presence of SHH. GCPs were electroporated with two different siRNAs against CK1 δ , and the mRNA levels were analyzed after 72 hr in vitro. Results shown are the averages of three independent experiments and are represented as the mean \pm SEM (* p < 0.05, ** p < 0.001, *** p < 0.001, **** p < 0.0001).

(Figures S2E and S2F). In contrast, CK1 α , ϵ , and γ 2 levels did not decrease during G1, suggesting that CK1 δ is a unique APC/C^{Cdh1} substrate among CK1 isoforms. Cyclin B1 levels decreased upon exit from mitosis (2 hr after nocodazole release), as determined by phospho-Histone H3 staining and PI-FACS (Figures S2E–S2G).

APC/C^{Cdh1} Controls CK1 δ in Cerebellar GCPs In Vivo

To test whether APC/C^{Cdh1} regulates CK1 δ ubiquitination and degradation in vivo, we conditionally deleted *Cdh1* (or *Fzr1*) in cerebellar GCPs by crossing *Tg(Atoh1-Cre)*⁺ mice with *Fzr1*^{fl/fl} mice (García-Higuera et al., 2008; Schüller et al., 2007). *Atoh1* is a bHLH transcription factor required for GCP neurogenesis (Ben-Arie et al., 1997); thus, *Tg(Atoh1-Cre)*⁺;*Fzr1*^{fl/fl} mice should have lower

overexpressed (Figures S2C and S2D). *Cdh1*-knockdown-mediated increase of CK1 δ also decreased Wee1 levels (Figure S2A). Thus, the relationships between *Cdh1* and CK1 δ and *Cdh1* and Wee1 were inverse.

APC/C^{Cdh1} substrate levels oscillate during the cell cycle, reaching a minimum during G1 when APC/C^{Cdh1} is most active (Penas et al., 2012). Thus, we predicted that if CK1 δ were an APC/C^{Cdh1} substrate, its levels would also decrease. To test this directly, we synchronized HeLa cells in mitosis via a well-established thymidine/nocodazole protocol, released them into G1 by washing away nocodazole, and monitored CK1 δ levels via western blot analysis (Figures S2E and S2F). Cell-cycle progression was monitored by PI-FACS (Figure S2G). CK1 δ levels were stable through mitosis and early G1 but decreased late in G1, 6 to 7 hr after release from nocodazole-induced arrest (Figure S2E). CK1 δ was undetectable before cells entered S phase

Cdh1 levels in GCPs relative to their wild-type or *Cre*⁻ littermates. *Cdh1* protein level was lower in GCPs purified from postnatal day (P) 7 *Tg(Atoh1-Cre)*⁺;*Fzr1*^{fl/fl} mice than in *Tg(Atoh1-Cre)*⁻;*Fzr1*^{fl/fl} mice (Figures 6A and 6B). Lower *Cdh1* levels also were associated with increased CK1 δ protein in *Tg(Atoh1-Cre)*⁺;*Fzr1*^{fl/fl} mice. These results suggest that CK1 δ is degraded via APC/C^{Cdh1} in GCPs in the developing mouse cerebellum. Although GCPs from *Tg(Atoh1-Cre)*⁺;*Fzr1*^{fl/fl} mice express higher levels of cell-cycle regulators (e.g., cyclin B1), their cerebella develop normally. This could be attributed to the incomplete knockout by *Atoh1-Cre* or compensatory mechanisms of *Cdc20*, another APC/C activator in GCPs.

We previously showed that APC/C^{Cdh1} targets substrates for degradation during the GCP cell cycle (Harmey et al., 2009). Because reducing CK1 δ levels or activity suppressed GCP expansion and APC/C^{Cdh1} substrates often induce cell-cycle

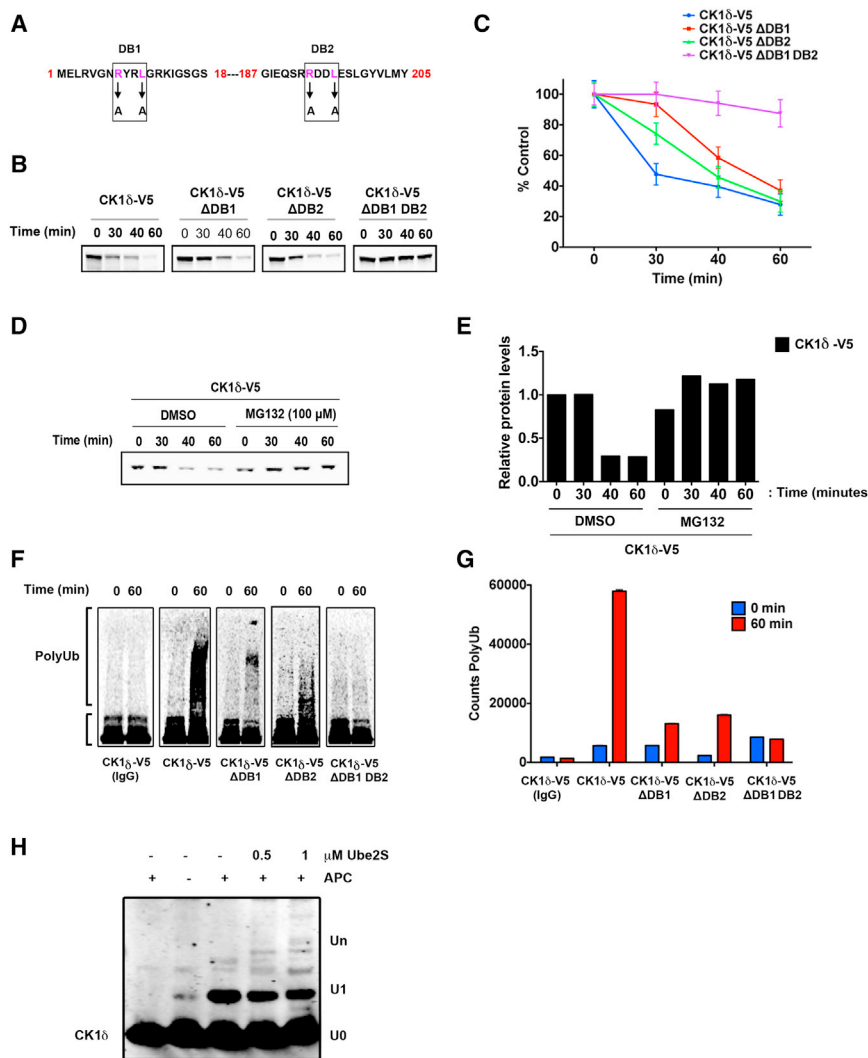


Figure 4. APC/C^{Cdh1} Induces CK1δ Ubiquitination and Degradation In Vitro

(A) Two destruction boxes (D-boxes) in human CK1δ, DB1 and DB2, were mutated by substituting alanine (A) for the corresponding arginine (R) and leucine (L) residues.

(B and C) Both D-boxes in CK1δ are required for proteolysis. (B) In vitro degradation assay indicating ³⁵S-labeled wild-type CK1δ-V5, DB1 mutant (CK1δ-V5 ΔDB1), DB2 mutant (CK1δ-V5 ΔDB2), and DB1 DB2 double mutant (CK1δ-V5 ΔDB1 DB2) after incubation in extracts prepared from HeLa cells in G1 is shown. Samples collected at the indicated time points were analyzed by autoradiography. (C) The quantification of (B); protein levels were measured in three separate experiments using Quantity One image analysis software (Bio-Rad). An unpaired t test was performed, and a p value of 0.01 was obtained.

(D) Autoradiogram indicating in vitro degradation of ³⁵S-labeled wild-type CK1δ-V5 in HeLa cell extracts at G1, in the presence or absence of the proteasome 26S inhibitor MG132 (100 μM), is shown.

(E) Quantification of CK1δ-V5 from (D) is shown. (F and G) Both D-boxes in CK1δ are required for efficient ubiquitination. (F) Autoradiogram of ³⁵S-labeled wild-type CK1δ-V5 and ΔDB1, ΔDB2, and ΔDB1 DB2 mutants after in vitro ubiquitination by anti-Cdc27 immunoprecipitates from HeLa cell extracts at G1 is shown. (G) The extent of poly-ubiquitination was quantified for the entire lane above the inputs by using Quantity One image analysis software. From three separate experiments, an unpaired t test was performed, and a p value of 0.005 was obtained. Results shown are the averages of three independent experiments and are represented as the mean ± SEM.

(H) Purified CK1δ and immunoprecipitated APC were incubated together in vitro, and the extent of ubiquitination was determined after SDS-PAGE and anti-CK1δ autoradiography.

transition, we asked whether CK1δ overexpression would stimulate GCP proliferation. Relative to V5 empty control vector, CK1δ-V5 or CK1δ-V5 ΔDB1 DB2 overexpression increased GCP proliferation (Figures 6C and 6D). These results suggest that controlling CK1δ levels is key to GCP cell-cycle transition. When GCPs were plated on poly-D-lysine/laminin-coated dishes, their CK1δ levels decreased. The cells then exited the cell cycle and differentiated. This reduction was similar to that observed for cyclin B1 (Figures 6E and 6F).

CK1δ Inhibition Decreases Medulloblastoma Growth Ex Vivo

CK1δ controls GCP proliferation in vitro and ex vivo, and GCPs are thought to give rise to some forms of medulloblastoma (Gibson et al., 2010; Kawachi et al., 2012; Schüller et al., 2008; Yang et al., 1999). Therefore, we tested whether CK1δ is a possible therapeutic target for medulloblastoma. First we measured CK1δ protein and mRNA levels in tumors obtained from mouse models of medulloblastoma (Figures 7A, 7B, S3A,

and S3B). CK1δ protein levels were higher in tumors derived from *Ptch1*^{+/-} or Myc mice (Goodrich et al., 1997; Kimura et al., 2005) than in untransformed GCPs (Figure 7A). Higher protein levels were not accompanied by increased *Csnk1d* (CK1δ) mRNA, indicating possible differential regulation of CK1δ in medulloblastoma relative to GCPs. Consistent with this notion, the level of the APC/C repressor Emi1 (FBXO31) in c-Myc (Myc)-derived tumors was higher (Figures S3C and S3D), indicating altered APC/C activity that could contribute to the difference in protein and RNA levels. Furthermore, increased CK1δ protein levels corresponded with decreased Wee1 levels (Figures 7A and 7B), suggesting that CK1δ-dependent control of Wee1 turnover also mediates medulloblastoma cell proliferation.

Ptch1 functions as an antagonist of SHH, which is a potent mitogen for cerebellar medulloblastoma (Wechsler-Reya and Scott, 1999, 2001). *Ptch1* mutation constitutively activates the SHH pathway and induces medulloblastoma tumors in 14% to 20% of mice. *Ptch1*^{+/-} mice have been used extensively to model human SHH-subgroup medulloblastoma.

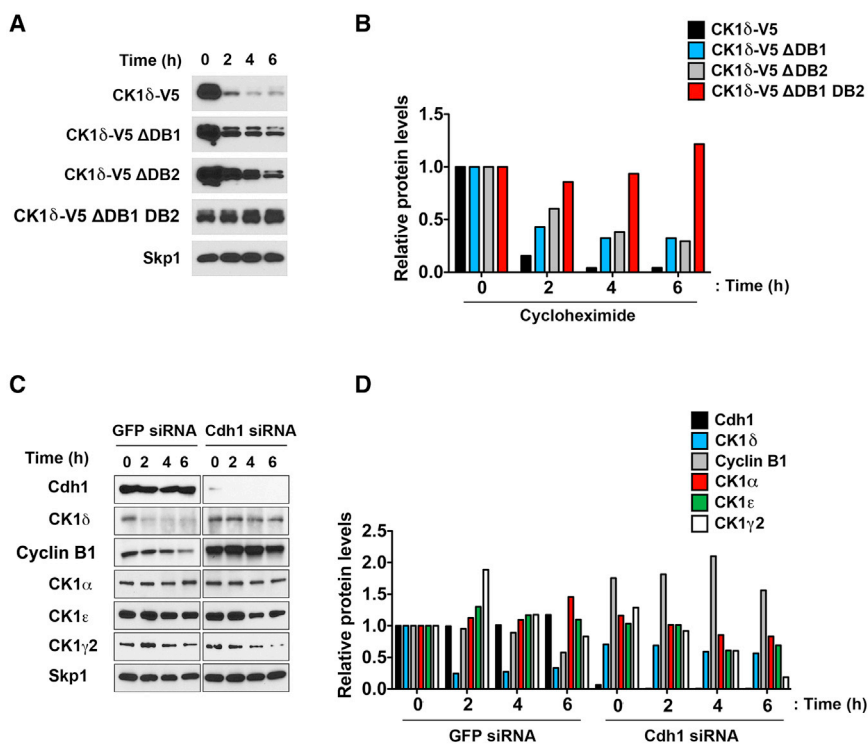


Figure 5. CK1δ Is Degraded by APC/C^{Cdh1} in a D-box-Dependent Manner

(A) CK1δ D-box mutations reduce the turnover of the protein in HeLa cells. HeLa cells transfected with the wild-type CK1δ-V5 or D-box mutants were treated with cycloheximide (100 μg/ml). Samples were then collected at the indicated time points and analyzed by immunoblotting.

(B) Quantification of (A) is shown.

(C) Cdh1 is required for CK1δ degradation. HeLa cells were transfected with the indicated siRNA, treated with cycloheximide for the indicated times, retrieved at the time points shown, and analyzed by immunoblotting.

(D) Quantification of (C) is shown.

CK1δ upregulation in mouse models of medulloblastoma suggests that it might be an attractive therapeutic target. To test this directly, we assessed the effectiveness of SR-1277 in reducing tumor growth in vivo. We implanted allografts from *Ptch1*^{+/-} mice into immunocompromised recipients and started treatment when the tumors reached a volume of 50 to 90 mm³. SR-1277 treatment significantly inhibited tumor growth (Figures 7C and 7D).

Human G3 medulloblastoma has been modeled recently in mice by overexpressing *Myc* (*c-Myc*) in neural progenitors purified from the cerebellum of P7 *Cdkn2c*^{-/-}; *Trp53*^{-/-} mice and transplanting those cells into the cortices of naive CD1 nude mice (Kawauchi et al., 2012). CK1δ protein was upregulated in G3 medulloblastoma cells (Figures 7A and 7B); therefore, we tested whether its inhibition reduces proliferation in this model. We treated mouse G3 medulloblastoma neurospheres with SR-1277 and measured the proliferation via an EdU-incorporation assay in vitro. SR-1277 inhibited proliferation, suggesting that CK1δ inhibition has potential as a therapeutic strategy for multiple human tumors. These results further indicate that human medulloblastoma cells also may respond to SR-1277. Treatment of two human medulloblastoma cell lines, DAOY and D283, with SR-1277 reduced proliferation (Figures 7G, S3E, and S3F). SR-1277 inhibited DAOY and D283 cell proliferation with the same efficacy as multiple compounds currently in clinical trials for cancer (Figures S3E and S3F). SR-1277 is 24% brain penetrant (Bibian et al., 2013); thus, it also reduced DAOY cell proliferation intracranially (Figures 7H and 7I). Collectively, these results validate CK1δ as a therapeutic target for human medulloblastoma.

GCP proliferation. Second, treatment of GCPs with specific CK1δ inhibitors dramatically reduced proliferation in vitro and ex vivo. Third, CK1δ overexpression had the opposite effect, namely, it stimulated GCP proliferation. Our studies further showed that CK1δ is targeted for proteolysis via the APC/C^{Cdh1} ubiquitin ligase, and conditional deletion of the APC/C activator *Cdh1* in cerebellar GCPs increased CK1δ levels. These findings also increase our understanding of developmental brain tumor formation. We observed high levels of CK1δ in a mouse model of medulloblastoma, and treatment with specific inhibitors of CK1δ dramatically reduced tumor growth. Together, these results suggest that CK1δ regulates normal GCP neurogenesis in the developing brain and medulloblastoma growth and that APC/C^{Cdh1}-dependent degradation of CK1δ controls the proliferation rate of normal cells and tumor cells.

Although CK1δ is expressed in several tissues (Löhler et al., 2009), its role in development has not been elucidated. Here we demonstrate that CK1δ is required for the proliferation and expansion of GCPs, one of two principal classes of neurons in the developing cerebellum. Decreasing CK1δ levels lowered cyclin levels. Furthermore, consistent with decreased cell-cycle transition in the absence of CK1δ, inhibition or knockdown of CK1δ decreased the levels of the main effectors of the SHH pathway, which is an important mitogenic pathway for GCP expansion during cerebellar development (Salero and Hatten, 2007; Wechsler-Reya and Scott, 1999).

Centrosomal CK1δ mediates the formation of primary cilia, an organelle that functions in WNT and SHH signal transduction (Greer et al., 2014). In fact, several proteins that localize to primary cilia or are involved in ciliogenesis restrict cell proliferation by arresting cells at G1/S, G2/M, or both phases. Therefore,

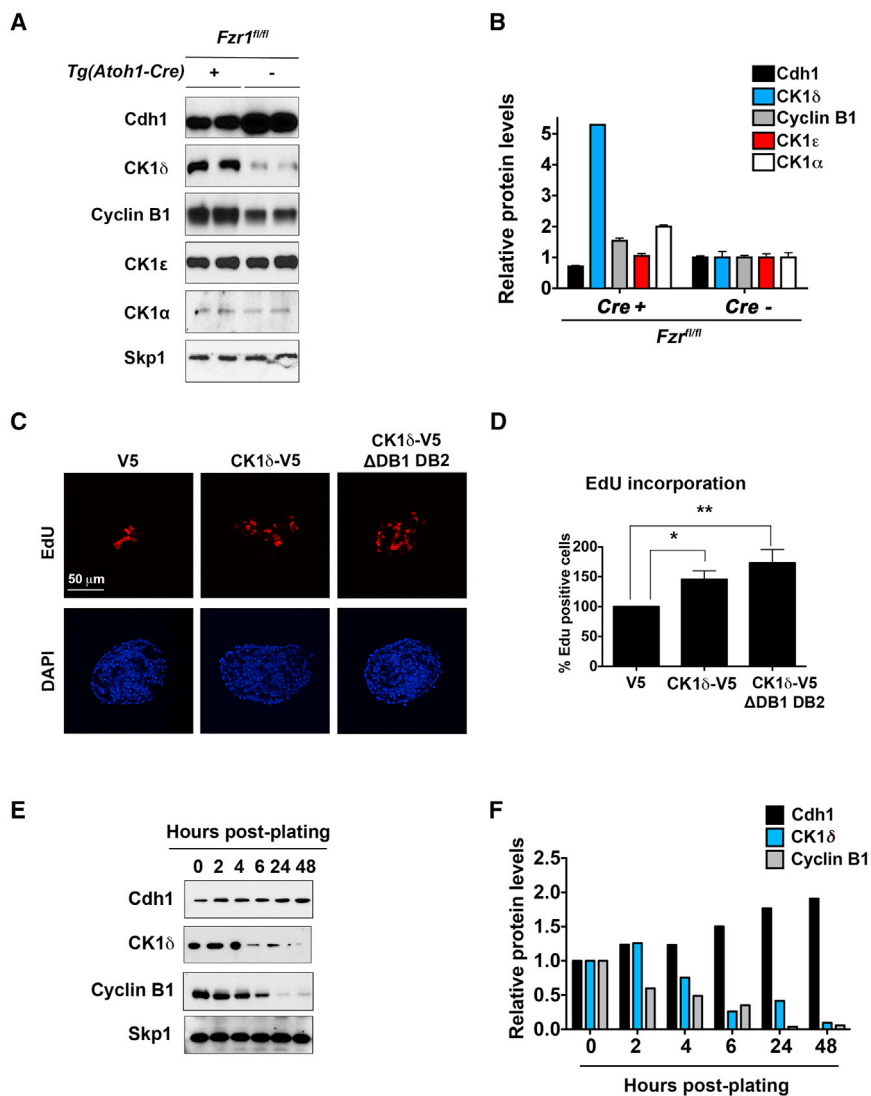


Figure 6. Conditional Deletion of *Fzr1* in the Cerebellum Increases CK1 δ Levels

(A) Immunoblot analysis shows that the levels of cyclin B1 and CK1 δ , but not CK1 ϵ , are higher in GCPs purified from *Fzr1*-knockout mice than in those from control mice. Protein extracts were made directly after GCP purification. GCPs were not maintained in culture.

(B) Quantification of (A) is shown.

(C) Overexpression of CK1 δ -V5 in purified GCPs increases cell proliferation, as indicated by the amount of EdU-positive cells (red) in the presence of SHH (75 ng/ml). EdU incorporation into cells electroporated with the CK1 δ -V5 or CK1 δ -V5 Δ DB1 DB2 construct was normalized to that of cells electroporated with the empty control vector (V5).

(D) Quantification of (C) is shown.

(E) CK1 δ levels decrease during GCP cell-cycle exit. Representative western blotting of CK1 δ , Cdh1, cyclin B1, and the loading control Skp1 is shown.

(F) Quantification of (E). Results shown are averages of three independent experiments and are represented as the mean \pm SEM (* p < 0.05, ** p < 0.001).

CK1 δ deletion or inhibition may affect the cell cycle by disrupting ciliogenesis. Another possibility is that, after CK1 δ deletion or inhibition, increased levels of Wee1 induce cell-cycle arrest (Penas et al., 2014). We found that CK1 δ overexpression and depletion had the opposite effects on Wee1 levels. Namely, CK1 δ overexpression reduced the level of Wee1, and CK1 δ depletion increased it. Thus, modulating CK1 δ levels appears to directly control Wee1 turnover, which is important for transitioning through the S and G2/M phases.

The present study shows that APC/C^{Cdh1} complex-mediated degradation controls CK1 δ levels in GCPs. Conditional deletion of *Fzr1*, which encodes Cdh1, in GCPs of the developing cerebellum increased the levels of CK1 δ , but not CK1 α or CK1 ϵ , and overexpression of CK1 δ increased GCP proliferation. Although we demonstrated that APC/C^{Cdh1} regulates CK1 δ levels, we did not detect a difference in EdU incorporation in the *Fzr1*-knockout mice relative to their wild-type littermates, which may be due to incomplete deletion of *Fzr1* or compensa-

tion from Cdc20, another APC/C activator. CK1 δ is the only CK1 isoform that is targeted by APC/C^{Cdh1} in the developing cerebellum. How APC/C^{Cdh1} acquires specificity for the CK1 δ isoform in the context of GCP proliferation is unknown, since other CK1 isoforms also contain D-boxes that could potentially mediate turnover via APC/C^{Cdh1}. However, CK1 δ is the only CK1 isoform that contains an N-terminal D-box motif; the other CK1 members may require activation of upstream signaling pathways to be recognized by APC/C^{Cdh1}. The identi-

fication of GCP-specific interactors or substrates also may shed light on the mechanism by which APC/C^{Cdh1} regulates CK1 δ levels during cell-cycle progression in this system.

CK1 δ may be deregulated in medulloblastoma. CK1 δ protein level was higher in two different types of medulloblastoma, *Ptch1*^{-/-}-driven and Myc-driven medulloblastomas, which model SHH and G3 subtypes of human medulloblastoma, respectively. Increased CK1 δ expression in medulloblastoma is consistent with previous findings of elevated CK1 δ levels in adenocarcinoma (Brockschmidt et al., 2008) and breast cancer (Knippschild et al., 2005). Thus, CK1 δ is an attractive therapeutic target because highly specific, small-molecule inhibitors can be generated against it (Bischof et al., 2012; Rena et al., 2004). We developed and characterized the highly selective CK1 δ small-molecule inhibitor SR-1277, which reduced medulloblastoma tumor growth in vivo. SR-1277 decreased the proliferation of medulloblastoma cells that either contained alterations in SHH signaling or overexpressed Myc. *C-MYC* expression has been

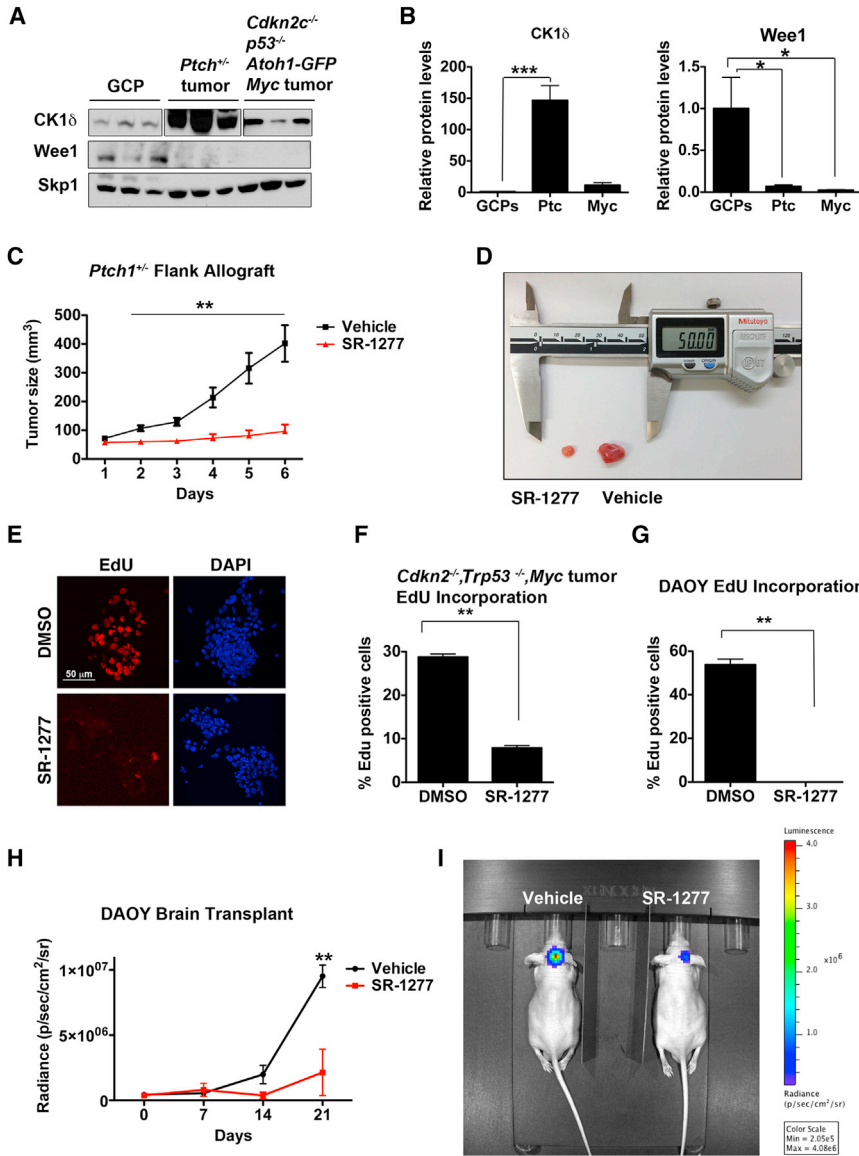


Figure 7. Murine Medulloblastoma Cells Express Elevated Levels of CK1δ, the Inhibition of Which Reduces Tumor Growth In Vivo

(A) CK1δ protein is overexpressed in *Ptch*^{+/+}, *Cdkn2c*^{-/-}, *Trp53*^{-/-}, and *c-Myc* tumors, whereas Wee1 is downregulated. Skp1 was used as a loading control.

(B) Quantification of (A) is shown.

(C and D) SR-1277 decreases proliferation of *Ptch*^{+/+} allograft tumors. *Ptch*^{+/+} tumor cells were injected subcutaneously into mice. Once the tumor reached a volume of 50 to 90 mm³, treatment with vehicle or SR-1277 (20 mg/kg, twice daily) was initiated. (C) Tumor size was quantified in four samples for each time point, and the averages are shown. (D) An image shows representative SR-1277-treated (left) and vehicle-treated (right) tumors.

(E) Proliferation of *Cdkn2c*^{-/-}, *Trp53*^{-/-}, and *c-Myc* tumor cells is reduced in the presence of SR-1277. (F) Quantification of EdU incorporation into *Cdkn2c*^{-/-}, *Trp53*^{-/-}, or *c-Myc* tumor cells after DMSO or SR-1277 treatment is shown.

(G) EdU-incorporation assay shows that proliferation of DAOY cells is reduced in the presence of SR-1277 (500 nM).

(H and I) SR-1277 also reduces the intracranial growth of DAOY cells. (H) Twelve days after mice were transplanted with DAOY tumor cells, D-luciferin was administered intraperitoneally and bioluminescence was measured. (I) Fluorescence imaging of representative mice in which DAOY cells were implanted intracranially and then treated with SR-1277 (20 mg/kg, twice daily) or vehicle for 21 days. Bioluminescence was quantified from the encircled regions that enclose the entire tumor. Results shown are the means ± SEM of three independent experiments (*p < 0.05, **p < 0.001, ***p < 0.001).

EXPERIMENTAL PROCEDURES

Animal Husbandry

This study was approved by the Institutional Animal Care and Use Committees of the University of Miami, The Rockefeller University, Scripps Florida, and St. Jude Children's Research Hospital (see [Supplemental Experimental Procedures](#)).

ida, and St. Jude Children's Research Hospital (see [Supplemental Experimental Procedures](#)).

GCP Culture System

GCPs were purified from cerebellar cortices of P6 CD-1 (Jackson Laboratory), *Tg(Atoh1-Cre);Csnk1d^{fl/fl}*, or *Tg(Atoh1-Cre);Fzr1^{fl/fl}* mice by using Percoll gradient sedimentation (see [Supplemental Experimental Procedures](#)). For proliferation assays, GCPs were suspended in culture medium; for cell-cycle exit and differentiation assays, GCPs were plated in poly-D-lysine/laminin-coated plates. GCPs were treated with compounds and then subsequently used for apoptosis, ³H-thymidine-incorporation, or EdU-proliferation assays; fixed for FACS analysis; or lysed to obtain protein for western blot analysis or RNA for qRT-PCR analysis (see [Supplemental Experimental Procedures](#)).

Plasmids, siRNAs, and Site-Directed Mutagenesis

The CK1δ-V5 construct was generated by cloning the full-length *Csnk1d* gene from the Gateway donor vector pDONR223-CSNK1D (Addgene) into the Gateway destination vector pcDNA-DEST40 (Invitrogen). The siRNAs and

linked to poor outcome in multiple studies of patients with medulloblastoma (Gilbertson and Ellison, 2008; Hatten and Rousel, 2011); thus, it will be important to study the effectiveness of SR-1277 treatment for human G3 medulloblastoma.

In summary, the present study showed that CK1δ regulates cerebellar GCP proliferation, suggesting an important role of CK1 in brain development. In addition, CK1δ may influence the malignant transformation of GCPs, as medulloblastoma growth also was related to CK1δ levels. Furthermore, our results demonstrate that CK1δ is targeted for proteolysis via the APC/C^{Cdh1} ubiquitin ligase, suggesting that APC/C^{Cdh1} regulates CK1δ in proliferating cells. They also indicate that measuring CK1δ protein levels in tumors will be essential for determining responsiveness to CK1δ-inhibitor treatment, as APC/C^{Cdh1} is deregulated in various cancers (García-Higuera et al., 2008; Penas et al., 2012).

primers used for cloning are listed in the [Supplemental Experimental Procedures](#).

HeLa Cell Culture System

HeLa cells were transfected with plasmids by using TransIT-LT1 transfection reagent (Mirus Bio) or with siRNAs using DharmaFECT 1 transfection reagent (Thermo Scientific), per each manufacturer's instructions. HeLa cells were lysed for in vitro cyclohexamide degradation and ubiquitination assays, to obtain protein for western blot analysis or RNA for qRT-PCR analysis, or synchronized and fixed for flow cytometric analysis (see [Supplemental Experimental Procedures](#)).

Organotypic Slice Cultures and Proliferation Assays

Cerebella were isolated from P8 mice, and 250- μ m sagittal slices of cerebellar cortex were cut using a Leica VT1000S vibratome. Slices were then plated on Millipore culture inserts in six-well culture dishes (Falcon) containing 1.5 ml serum-free medium. Slices were treated with compounds and EdU-incorporation assay or immunohistochemical analyses performed (see [Supplemental Experimental Procedures](#)).

In Vivo Allograft

Ptch1^{+/-} tumor cells in matrigel (BD Biosciences) solution were injected subcutaneously into the right flank of a NU-Foxn1nu mouse (Charles River Laboratories). Treatment with SR-1277 began when tumors reached 50 to 90 mm³ (see [Supplemental Experimental Procedures](#)).

Murine G3 Medulloblastoma Neurospheres in Culture

Tumor cells were maintained in culture as previously described ([Kawauchi et al., 2012](#); [Supplemental Experimental Procedures](#)). They were treated with SR-1277 and EdU-proliferation assays were performed.

Transduction and Transplantation of DAOY Cells

DAOY cells were transduced with firefly luciferase lentivirus (Capital Biosciences). Stable clones were then selected with puromycin (see [Supplemental Experimental Procedures](#)), and 10⁵ labeled DAOY cells were injected into the ventral pallidum of NCr nude mice (Taconic). After 10 days, tumor growth was monitored weekly by bioluminescence imaging of the pallidum (see [Supplemental Experimental Procedures](#)).

Statistical Analyses

All experiments were conducted independently and at least in triplicate. Statistical analysis was performed with Prism software (GraphPad). Data in [Figures 1D, 1E, 1G, 2F, 3A, 3B, S1A, S1B](#), and 6D were analyzed via one-way ANOVA followed by Bonferroni multiple comparisons test ($p < 0.5$); that in [Figures 1F](#) and [2G](#), two-way ANOVA followed by Bonferroni multiple comparisons test ($p < 0.5$); that in [Figures 2D, 7F](#), and [7G](#), paired t test ($p < 0.5$); and that in [Figures 1B, 7B, 7C](#), and [7H](#), one-way ANOVA followed by Dunnett multiple comparisons test ($p < 0.5$).

SUPPLEMENTAL INFORMATION

Supplemental Information includes Supplemental Experimental Procedures and three figures and can be found with this article online at <http://dx.doi.org/10.1016/j.celrep.2015.03.016>.

AUTHOR CONTRIBUTIONS

C.P., E.-E.G., Y.F., V.R., M.D., W.W., M.E.M., R.J.R., M.B., D.K., D.F., J.-L.H., J.L., and B.L. performed the experiments and analyzed the data. N.G.A., M.M., D.J.R., M.F.R., W.R.R., and M.E.H. designed and interpreted the experiments. C.P., E.-E.G., W.R.R., M.E.H., and N.G.A. wrote the paper. All authors reviewed and edited the paper.

ACKNOWLEDGMENTS

We thank Dr. David Rowitch (University of California, San Francisco) for providing the *Atoh1-Cre* deleter line and Dr. Marc Kirschner for helpful discus-

sions and critical reading of the manuscript. We also thank all members of the Center for Therapeutic Innovation (University of Miami) and the Department of Cancer Biology (Scripps Florida) for helpful suggestions. We thank Dr. Angela MacArthur and the Department of Scientific Editing at St. Jude Children's Research Hospital for helpful suggestions. This work was supported by R21 NS056991 (N.G.A.), R01NS067289 (N.G.A. and M.E.H.), NIH grant NCI CA-096832 (M.F.R.), NIH Molecular Library Screening Center Network grant U54MH074404 (W.R.R., Hugh Rosen, PI), Core Grant CA-021765 (M.F.R., D.K., and D.F.), the Anderson Fellowship (D.K.), and the American Lebanese-Syrian Associated Charities (ALSAC) of St. Jude Children's Research Hospital (M.F.R., D.K., and D.F.) as well as the Spanish Ministerio de Economía y Competitividad (MINECO, SAF2012-38215), Fundación Ramón Areces, Comunidad de Madrid (S2010/BMD-2470), and the European Union Seventh Framework Programme (MitoSys project; HEALTH-F5-2010-241548) (M.M.).

Received: July 11, 2014

Revised: December 23, 2014

Accepted: March 5, 2015

Published: April 2, 2015

REFERENCES

- Barford, D. (2011). Structure, function and mechanism of the anaphase promoting complex (APC/C). *Q. Rev. Biophys.* 44, 153–190.
- Behrend, L., Stöter, M., Kurth, M., Rutter, G., Heukeshoven, J., Deppert, W., and Knippschild, U. (2000). Interaction of casein kinase 1 delta (CK1delta) with post-Golgi structures, microtubules and the spindle apparatus. *Eur. J. Cell Biol.* 79, 240–251.
- Ben-Arie, N., Bellen, H.J., Armstrong, D.L., McCall, A.E., Gordadze, P.R., Guo, Q., Matzuk, M.M., and Zoghbi, H.Y. (1997). Math1 is essential for genesis of cerebellar granule neurons. *Nature* 390, 169–172.
- Beyaert, R., Vanhaesebroeck, B., Declercq, W., Van Lint, J., Vandenabele, P., Agostinis, P., Vandenheede, J.R., and Fiers, W. (1995). Casein kinase-1 phosphorylates the p75 tumor necrosis factor receptor and negatively regulates tumor necrosis factor signaling for apoptosis. *J. Biol. Chem.* 270, 23293–23299.
- Bibian, M., Rahaim, R.J., Choi, J.Y., Noguchi, Y., Schürer, S., Chen, W., Nakanishi, S., Licht, K., Rosenberg, L.H., Li, L., et al. (2013). Development of highly selective casein kinase 1 $\delta/1\epsilon$ (CK1 δ/ϵ) inhibitors with potent antiproliferative properties. *Bioorg. Med. Chem. Lett.* 23, 4374–4380.
- Bischof, J., Leban, J., Zaja, M., Grothey, A., Radunsky, B., Othersen, O., Strobl, S., Vitt, D., and Knippschild, U. (2012). 2-Benzamido-N-(1H-benzo[d]imidazol-2-yl)thiazole-4-carboxamide derivatives as potent inhibitors of CK1 δ/ϵ . *Amino Acids* 43, 1577–1591.
- Brockschmidt, C., Hirner, H., Huber, N., Eismann, T., Hillenbrand, A., Giamas, G., Radunsky, B., Ammerpohl, O., Böhm, B., Henne-Bruns, D., et al. (2008). Anti-apoptotic and growth-stimulatory functions of CK1 delta and epsilon in ductal adenocarcinoma of the pancreas are inhibited by IC261 in vitro and in vivo. *Gut* 57, 799–806.
- Cheong, J.K., and Virshup, D.M. (2011). Casein kinase 1: complexity in the family. *Int. J. Biochem. Cell Biol.* 43, 465–469.
- Cho, Y.J., Tsherniak, A., Tamayo, P., Santagata, S., Ligon, A., Greulich, H., Berhoukim, R., Amani, V., Goumnerova, L., Eberhart, C.G., et al. (2011). Integrative genomic analysis of medulloblastoma identifies a molecular subgroup that drives poor clinical outcome. *J. Clin. Oncol.* 29, 1424–1430.
- Choi, E., Dial, J.M., Jeong, D.E., and Hall, M.C. (2008). Unique D box and KEN box sequences limit ubiquitination of Acm1 and promote pseudosubstrate inhibition of the anaphase-promoting complex. *J. Biol. Chem.* 283, 23701–23710.
- Desagher, S., Osen-Sand, A., Montessuit, S., Magnenat, E., Vilbois, F., Hochmann, A., Journot, L., Antonsson, B., and Martinou, J.C. (2001). Phosphorylation of bid by casein kinases I and II regulates its cleavage by caspase 8. *Mol. Cell* 8, 601–611.
- Edmondson, J.C., and Hatten, M.E. (1987). Glial-guided granule neuron migration in vitro: a high-resolution time-lapse video microscopic study. *J. Neurosci.* 7, 1928–1934.

- Ellison, D.W., Dalton, J., Kocak, M., Nicholson, S.L., Fraga, C., Neale, G., Kenney, A.M., Brat, D.J., Perry, A., Yong, W.H., et al. (2011). Medulloblastoma: clinicopathological correlates of SHH, WNT, and non-SHH/WNT molecular subgroups. *Acta Neuropathol.* *121*, 381–396.
- Evans, D.G., Farnon, P.A., Burnell, L.D., Gattamaneni, H.R., and Birch, J.M. (1991). The incidence of Gorlin syndrome in 173 consecutive cases of medulloblastoma. *Br. J. Cancer* *64*, 959–961.
- García-Higuera, I., Machado, E., Dubus, P., Cañamero, M., Méndez, J., Moreno, S., and Malumbres, M. (2008). Genomic stability and tumour suppression by the APC/C cofactor Cdh1. *Nat. Cell Biol.* *10*, 802–811.
- Gault, W.J., Olguin, P., Weber, U., and Mlodzik, M. (2012). *Drosophila* CK1- γ , gilgamesh, controls PCP-mediated morphogenesis through regulation of vesicle trafficking. *J. Cell Biol.* *196*, 605–621.
- Gibson, P., Tong, Y., Robinson, G., Thompson, M.C., Currie, D.S., Eden, C., Kranenburg, T.A., Hogg, T., Poppleton, H., Martin, J., et al. (2010). Subtypes of medulloblastoma have distinct developmental origins. *Nature* *468*, 1095–1099.
- Gilbertson, R.J., and Ellison, D.W. (2008). The origins of medulloblastoma subtypes. *Annu. Rev. Pathol.* *3*, 341–365.
- Goodrich, L.V., Milenković, L., Higgins, K.M., and Scott, M.P. (1997). Altered neural cell fates and medulloblastoma in mouse patched mutants. *Science* *277*, 1109–1113.
- Greer, Y.E., Westlake, C.J., Gao, B., Bharti, K., Shiba, Y., Xavier, C.P., Pazour, G.J., Yang, Y., and Rubin, J.S. (2014). Casein kinase 1 δ functions at the centrosome and Golgi to promote ciliogenesis. *Mol. Biol. Cell* *25*, 1629–1640.
- Gross, S.D., and Anderson, R.A. (1998). Casein kinase I: spatial organization and positioning of a multifunctional protein kinase family. *Cell. Signal.* *10*, 699–711.
- Hallahan, A.R., Pritchard, J.I., Hansen, S., Benson, M., Stoeck, J., Hatton, B.A., Russell, T.L., Ellenbogen, R.G., Bernstein, I.D., Beachy, P.A., and Olson, J.M. (2004). The SmoA1 mouse model reveals that notch signaling is critical for the growth and survival of sonic hedgehog-induced medulloblastomas. *Cancer Res.* *64*, 7794–7800.
- Harmey, D., Smith, A., Simanski, S., Moussa, C.Z., and Ayad, N.G. (2009). The anaphase promoting complex induces substrate degradation during neuronal differentiation. *J. Biol. Chem.* *284*, 4317–4323.
- Hatten, M.E., and Roussel, M.F. (2011). Development and cancer of the cerebellum. *Trends Neurosci.* *34*, 134–142.
- Jones, D.T., Jäger, N., Kool, M., Zichner, T., Hutter, B., Sultan, M., Cho, Y.J., Pugh, T.J., Hovestadt, V., Stütz, A.M., et al. (2012). Dissecting the genomic complexity underlying medulloblastoma. *Nature* *488*, 100–105.
- Kawauchi, D., Robinson, G., Uziel, T., Gibson, P., Rehg, J., Gao, C., Finkelstein, D., Qu, C., Pounds, S., Ellison, D.W., et al. (2012). A mouse model of the most aggressive subgroup of human medulloblastoma. *Cancer Cell* *21*, 168–180.
- Kimura, H., Stephen, D., Joyner, A., and Curran, T. (2005). Gli1 is important for medulloblastoma formation in Ptc1 $^{-/-}$ mice. *Oncogene* *24*, 4026–4036.
- King, R.W., Glotzer, M., and Kirschner, M.W. (1996). Mutagenic analysis of the destruction signal of mitotic cyclins and structural characterization of ubiquitinated intermediates. *Mol. Biol. Cell* *7*, 1343–1357.
- Kisselev, A.F., van der Linden, W.A., and Overkleeft, H.S. (2012). Proteasome inhibitors: an expanding army attacking a unique target. *Chem. Biol.* *19*, 99–115.
- Knippschild, U., Gocht, A., Wolff, S., Huber, N., Löhler, J., and Stöter, M. (2005). The casein kinase 1 family: participation in multiple cellular processes in eukaryotes. *Cell. Signal.* *17*, 675–689.
- Listovsky, T., Oren, Y.S., Yudkovsky, Y., Mahbubani, H.M., Weiss, A.M., Lebediker, M., and Brandeis, M. (2004). Mammalian Cdh1/Fzr mediates its own degradation. *EMBO J.* *23*, 1619–1626.
- Löhler, J., Hirner, H., Schmidt, B., Kramer, K., Fischer, D., Thal, D.R., Leithäuser, F., and Knippschild, U. (2009). Immunohistochemical characterisation of cell-type specific expression of CK1 δ in various tissues of young adult BALB/c mice. *PLoS ONE* *4*, e4174.
- Northcott, P.A., Korshunov, A., Witt, H., Hielscher, T., Eberhart, C.G., Mack, S., Bouffet, E., Clifford, S.C., Hawkins, C.E., French, P., et al. (2011). Medulloblastoma comprises four distinct molecular variants. *J. Clin. Oncol.* *29*, 1408–1414.
- Northcott, P.A., Shih, D.J., Peacock, J., Garzia, L., Morrissy, A.S., Zichner, T., Stütz, A.M., Korshunov, A., Reimand, J., Schumacher, S.E., et al. (2012). Subgroup-specific structural variation across 1,000 medulloblastoma genomes. *Nature* *488*, 49–56.
- Owens, T.J., and Hoyt, M.A. (2005). The D box asserts itself. *Mol. Cell* *18*, 611–612.
- Owens, L., Simanski, S., Squire, C., Smith, A., Cartzendafner, J., Cavett, V., Caldwell Busby, J., Sato, T., and Ayad, N.G. (2010). Activation domain-dependent degradation of somatic Wee1 kinase. *J. Biol. Chem.* *285*, 6761–6769.
- Penas, C., Ramachandran, V., and Ayad, N.G. (2012). The APC/C ubiquitin ligase: from cell biology to tumorigenesis. *Front. Oncol.* *1*, 60.
- Penas, C., Ramachandran, V., Simanski, S., Lee, C., Madoux, F., Rahaim, R.J., Chauhan, R., Barnaby, O., Schurer, S., Hodder, P., et al. (2014). Casein kinase 1 δ -dependent Wee1 protein degradation. *J. Biol. Chem.* *289*, 18893–18903.
- Petronczki, M., Matos, J., Mori, S., Gregan, J., Bogdanova, A., Schwickart, M., Mechtler, K., Shirahige, K., Zachariae, W., and Nasmyth, K. (2006). Monopolar attachment of sister kinetochores at meiosis I requires casein kinase 1. *Cell* *126*, 1049–1064.
- Pfister, S., Remke, M., Benner, A., Mendorzyk, F., Toedt, G., Felsberg, J., Wittmann, A., Devens, F., Gerber, N.U., Joos, S., et al. (2009). Outcome prediction in pediatric medulloblastoma based on DNA copy-number aberrations of chromosomes 6q and 17q and the MYC and MYCN loci. *J. Clin. Oncol.* *27*, 1627–1636.
- Price, M.A. (2006). CKI, there's more than one: casein kinase I family members in Wnt and Hedgehog signaling. *Genes Dev.* *20*, 399–410.
- Pugh, T.J., Weeraratne, S.D., Archer, T.C., Pomeranz Krummel, D.A., Auclair, D., Bochicchio, J., Carneiro, M.O., Carter, S.L., Cibulskis, K., Erlich, R.L., et al. (2012). Medulloblastoma exome sequencing uncovers subtype-specific somatic mutations. *Nature* *488*, 106–110.
- Rakic, P. (1972). Mode of cell migration to the superficial layers of fetal monkey neocortex. *J. Comp. Neurol.* *145*, 61–83.
- Rena, G., Bain, J., Elliott, M., and Cohen, P. (2004). D4476, a cell-permeant inhibitor of CK1, suppresses the site-specific phosphorylation and nuclear exclusion of FOXO1a. *EMBO Rep.* *5*, 60–65.
- Robinson, G., Parker, M., Kranenburg, T.A., Lu, C., Chen, X., Ding, L., Phoenix, T.N., Hedlund, E., Wei, L., Zhu, X., et al. (2012). Novel mutations target distinct subgroups of medulloblastoma. *Nature* *488*, 43–48.
- Roussel, M.F., and Hatten, M.E. (2011). Cerebellum development and medulloblastoma. *Curr. Top. Dev. Biol.* *94*, 235–282.
- Rowles, J., Slaughter, C., Moomaw, C., Hsu, J., and Cobb, M.H. (1991). Purification of casein kinase I and isolation of cDNAs encoding multiple casein kinase I-like enzymes. *Proc. Natl. Acad. Sci. USA* *88*, 9548–9552.
- Salero, E., and Hatten, M.E. (2007). Differentiation of ES cells into cerebellar neurons. *Proc. Natl. Acad. Sci. USA* *104*, 2997–3002.
- Schüller, U., Zhao, Q., Godinho, S.A., Heine, V.M., Medema, R.H., Pellman, D., and Rowitch, D.H. (2007). Forkhead transcription factor FoxM1 regulates mitotic entry and prevents spindle defects in cerebellar granule neuron precursors. *Mol. Cell. Biol.* *27*, 8259–8270.
- Schüller, U., Heine, V.M., Mao, J., Kho, A.T., Dillon, A.K., Han, Y.G., Huillard, E., Sun, T., Ligon, A.H., Qian, Y., et al. (2008). Acquisition of granule neuron precursor identity is a critical determinant of progenitor cell competence to form Shh-induced medulloblastoma. *Cancer Cell* *14*, 123–134.
- Smith, A., Simanski, S., Fallahi, M., and Ayad, N.G. (2007). Redundant ubiquitin ligase activities regulate wee1 degradation and mitotic entry. *Cell Cycle* *6*, 2795–2799.
- Song, L., and Rape, M. (2011). Substrate-specific regulation of ubiquitination by the anaphase-promoting complex. *Cell Cycle* *10*, 52–56.

- Stewart, S., and Fang, G. (2005). Destruction box-dependent degradation of aurora B is mediated by the anaphase-promoting complex/cyclosome and Cdh1. *Cancer Res.* 65, 8730–8735.
- Svärd, J., Heby-Henricson, K., Persson-Lek, M., Rozell, B., Lauth, M., Bergström, A., Ericson, J., Toftgård, R., and Teglund, S. (2006). Genetic elimination of Suppressor of fused reveals an essential repressor function in the mammalian Hedgehog signaling pathway. *Dev. Cell* 10, 187–197.
- Taylor, M.D., Liu, L., Raffel, C., Hui, C.C., Mainprize, T.G., Zhang, X., Agatep, R., Chiappa, S., Gao, L., Lowrance, A., et al. (2002). Mutations in SUFU predispose to medulloblastoma. *Nat. Genet.* 31, 306–310.
- Tomoda, T., Bhatt, R.S., Kuroyanagi, H., Shirasawa, T., and Hatten, M.E. (1999). A mouse serine/threonine kinase homologous to *C. elegans* UNC51 functions in parallel fiber formation of cerebellar granule neurons. *Neuron* 24, 833–846.
- Vielhaber, E., and Virshup, D.M. (2001). Casein kinase I: from obscurity to center stage. *IUBMB Life* 51, 73–78.
- Watanabe, N., Arai, H., Nishihara, Y., Taniguchi, M., Watanabe, N., Hunter, T., and Osada, H. (2004). M-phase kinases induce phospho-dependent ubiquitination of somatic Wee1 by SCFbeta-TrCP. *Proc. Natl. Acad. Sci. USA* 101, 4419–4424.
- Watanabe, N., Arai, H., Iwasaki, J., Shiina, M., Ogata, K., Hunter, T., and Osada, H. (2005). Cyclin-dependent kinase (CDK) phosphorylation destabilizes somatic Wee1 via multiple pathways. *Proc. Natl. Acad. Sci. USA* 102, 11663–11668.
- Wechsler-Reya, R.J., and Scott, M.P. (1999). Control of neuronal precursor proliferation in the cerebellum by Sonic Hedgehog. *Neuron* 22, 103–114.
- Wechsler-Reya, R., and Scott, M.P. (2001). The developmental biology of brain tumors. *Annu. Rev. Neurosci.* 24, 385–428.
- Yang, X.W., Wynder, C., Doughty, M.L., and Heintz, N. (1999). BAC-mediated gene-dosage analysis reveals a role for Zfp1 (Ru49/Zfp38) in progenitor cell proliferation in cerebellum and skin. *Nat. Genet.* 22, 327–335.
- Yauch, R.L., Dijkgraaf, G.J., Alicke, B., Januario, T., Ahn, C.P., Holcomb, T., Pujara, K., Stinson, J., Callahan, C.A., Tang, T., et al. (2009). Smoothed mutation confers resistance to a Hedgehog pathway inhibitor in medulloblastoma. *Science* 326, 572–574.
- Zhai, L., Graves, P.R., Robinson, L.C., Italiano, M., Culbertson, M.R., Rowles, J., Cobb, M.H., DePaoli-Roach, A.A., and Roach, P.J. (1995). Casein kinase I gamma subfamily. Molecular cloning, expression, and characterization of three mammalian isoforms and complementation of defects in the *Saccharomyces cerevisiae* YCK genes. *J. Biol. Chem.* 270, 12717–12724.
- Zur, A., and Brandeis, M. (2002). Timing of APC/C substrate degradation is determined by fzy/fzr specificity of destruction boxes. *EMBO J.* 21, 4500–4510.